

# Analysis of $\Omega(2012)$ as a molecule in the chiral quark model

Xiaohuang Hu<sup>1</sup>, Jialun Ping<sup>+</sup>

*Department of Physics and Jiangsu Key Laboratory for Numerical Simulation of Large Scale Complex Systems, Nanjing Normal University, Nanjing 210023, P. R. China*

Inspired by the updated information on  $\Omega(2012)$  by the Belle Collaboration, we conduct a study of all possible  $S$ -wave pentaquark systems with quark contents  $sss\bar{q}$ ,  $q = u, d$  in a chiral quark model with the help of Gaussian expansion method. Channel coupling is also considered. The real-scaling method (stabilization method) is employed to identify and check the bound states and the genuine resonances. In addition, the decay widths of all resonances are given. The results show that  $\Omega(2012)$  can be interpreted as a  $\Xi^*K$  molecular state with quantum number of  $IJ^P = 0(\frac{3}{2})^-$ . Other resonances are obtained:  $\Xi^*K^*$  with  $IJ^P = 0(\frac{1}{2})^-$  and  $0(\frac{3}{2})^-$ ,  $\Omega\pi$  with  $IJ^P = 1(\frac{3}{2})^-$ . These pentaquark states is expected to be further verified in future experiments.

PACS numbers: 13.75.Cs, 12.39.Pn, 12.39.Jh

## I. INTRODUCTION

In 2018, an excited state of  $\Omega$  with a significance of  $8.6\sigma$  was reported in the  $K^-\Xi^0$  and  $K_S^0\Xi^-$  invariant mass distributions by the Belle Collaboration [1]. The measured mass and width of the state are  $2012.4 \pm 0.7 \pm 0.6$  MeV and  $6.4^{+2.5}_{-2.0} \pm 1.6$  MeV, respectively. Although the ground state  $\Omega(1672)$  was predicted in the quark model with the SU(3)-flavor symmetry by Gell-Mann [2] and Ne'eman [3] and discovered experimentally about half-century ago, only three  $\Omega$  excited states were listed in the Particle Data Group before the observation by the Belle Collaboration and there was little knowledge of the nature of them. Thus, the discovery of  $\Omega(2012)$  was mostly welcomed and triggered many theoretical investigations on the nature of the excited states of  $\Omega$ .

Before the observation of the state  $\Omega(2012)$ , a series of theoretical models and approaches, such as the quark model [4, 5], Skyrme model [6], lattice QCD [7], and large  $N_c$  [8], predicted that the masses of the first excited states of the  $\Omega(1672)$  are around 2.0 GeV, which are consistent with the result of the Belle Collaboration. Thus, it is reasonable to explain the  $\Omega(2012)$  as a good candidate for the first orbital excited state of  $\Omega(1672)$ . After the observation of  $\Omega(2012)$ , the subsequent theoretical researches have further explored the  $qqq$  picture of  $\Omega(2012)$  in the chiral quark model [9], QCD sum rule [10] and  $^3P^0$  model [11].

Nevertheless, the possibility of the pentaquark picture of  $\Omega(2012)$  cannot be excluded, considering its mass is very close to the threshold of the state  $\Xi^*\bar{K}$ . Actually, various theoretical approaches [12–15] have investigated the  $\Omega$  excited states in pentaquark picture before the Belle Collaborations's report. The observation of the  $\Omega(2012)$  also triggered a lot of theoretical work on this issue. In Ref. [16], the flavor SU(3) analysis was performed and found that the  $\Omega(2012)$  is likely to be a  $\Xi^*\bar{K}$  molecular state with  $J^P = \frac{3}{2}^-$ . Several work also interpreted the  $\Omega(2012)$  as a possible  $\Xi^*\bar{K}$  molecule state and further predicted a large decay width for the  $\Omega(2012) \rightarrow \Xi^*\bar{K} \rightarrow \Xi\pi\bar{K}$  [17–20].

In Ref. [21], the  $\Omega(2012)$  was a dynamically generated state from the coupled channel interactions of  $\Xi^*\bar{K}$  and  $\Omega\eta$  in  $S$  wave. Inspired by these theoretical results, a follow-up experiment was reported by the Belle Collaboration to measure three body decay of the  $\Omega(2012)$  to  $\Xi\pi\bar{K}$  [22]. The result showed that there is no significant  $\Omega(2012)$  signals in the  $\Xi\pi\bar{K}$  channel, which was in tension with molecular interpretation of the  $\Omega(2012)$ . Based on the measurements, Refs. [23, 24] revisited the  $\Omega(2012)$  by the coupled channel unitary approach in the molecular perspective, taking account of the interaction of the  $\Xi^*\bar{K}$ ,  $\Omega\eta$ , and  $\Xi K$  (D-wave) channels and indicated that the experimental properties of  $\Omega(2012)$  [22] can be easily accommodated. In the hadronic molecular approach, the state  $\Omega(2012)$  can be interpreted as the  $P$ -wave  $\Xi^*K$  molecule state with  $IJ^P = 0(\frac{1}{2})^+$  or  $\frac{3}{2}^+$  [25], while in Ref. [26], the  $\Omega(2012)$  was considered to contain the mixed  $\Xi^*\bar{K}$  and  $\Omega\eta$  hadronic components. In Ref. [27], a nonrelativistic constituent quark potential model was used and  $\Omega(2012)$  can be interpreted as a  $P$ -wave state with  $J^P = \frac{3}{2}^-$  in  $qqq$  picture. In Ref. [28], the  $\Omega(2012)$  was study in the nonleptonic weak decays of  $\Omega_c^0 \rightarrow \Xi^*\bar{K}\pi^+(\Omega\eta) \rightarrow (\Xi\bar{K})^-\pi^+$  and  $(\Xi\bar{K}\pi)^-\pi^+$  via final-state interactions of the  $\Xi^*\bar{K}$  and  $\Omega\eta$  pairs. However, the Belle Collaboration has revisited the measurement of  $\Omega(2012)^- \rightarrow \Xi(1530)^0 K^- \rightarrow \Xi^-\pi^+ K^-$  and update the measurements of  $\Omega(2012)^- \rightarrow \Xi^0 K^-$  and  $\Omega(2012)^- \rightarrow \Xi^- K_S^0$  with improved selection criteria very recently [29]. The results show that the ratio of the branching fraction for the resonant three-body decay to that for the two-body decay to  $\Xi\bar{K}$  is  $0.97 \pm 0.24 \pm 0.07$ , consistent with the molecular picture of  $\Omega(2012)$ . The conclusion is in contrast to the previous study [22] and suggests that  $\Omega(2012)$  can be interpreted as a molecular state.

The state  $\Omega(2012)$  was also investigated in the framework of chiral quark model (ChQM) and quark delocalization color screening model (QDCSM) before in our group [30]. However, there is a mass inversion of  $\Xi^*\bar{K}$  channel and  $\Omega\eta$  channel due to the single Gaussian approximation in constructing the wave functions of

hadrons. In the Rayleigh-Ritz variational method, the basis expansion of the trial wave function is significant. In this work, Gaussian expansion method (GEM) [31] in which each relative motion in the system is expanded in terms of Gaussian basis functions whose sizes are taken in geometric progression, is adopted. The GEM has proven to be an accurate and universal few-body calculation method [32–35] and we hope to solve the previous problem of mass inversion by this method and to describe the hadron spectrum better. The constituent chiral quark model will still be employed to investigate all possible  $S$ -wave pentaquark systems for  $\Omega(2012)$ , considering the channel coupling interactions. After considering all possible configurations of color, spin and flavor degrees of freedom, we can identify the structures of these systems. Finally, with the help of “real scaling method” [36–38], we can confirm the bound states and the genuine resonances and obtain decay widths of resonances.

The paper is organized as follow. After introduction, details of ChQM and GEM are introduced in Section II. In Section III, we present the numerical results and a method of finding and calculating the decay width of the genuine resonance state (“real scaling method”). Finally, We give a brief summary of this work in the last section.

## II. CHIRAL QUARK MODEL AND WAVE FUNCTIONS

When it comes to multi-quark candidates observed by experiments, QCD-inspired quark model approach is still one of the most common tool for describing them. The chiral quark model has become one of the most effective approaches to describe hadron spectra, hadron-hadron interactions and multi-quark states [39]. The general form of five-body Hamiltonian in the model is given as follows:

$$H = \sum_{i=1}^5 \left( m_i + \frac{p_i^2}{2m_i} \right) - T_{CM} + \sum_{j>i=1}^5 [V_{CON}(\mathbf{r}_{ij}) + V_{OGE}(\mathbf{r}_{ij}) + V_{GBE}(\mathbf{r}_{ij})], \quad (1)$$

where  $m_i$  is the constituent mass of quark (antiquark),  $\mathbf{p}_i$  is momentum of quark and  $T_{cm}$  is the kinetic energy of the center-of mass motion. Due to the fact that a nearly massless current light quark acquires a dynamical, momentum dependent mass (so-called constituent quark mass) for its interaction with the gluon medium, ChQM contains color confinement potential, one-gluon exchange potential (OGE) and Goldstone boson exchange potentials (GBE). These three potentials reveal the most relevant features of QCD at low energy regime: confinement, asymptotic freedom and chiral symmetry spontaneous breaking.

In this work, we are interested in the low-lying pentaquark systems of  $S$ -wave composed of  $sss\bar{q}\bar{q}$ ,  $q = u, d$ .

Hence, only the central part of the quark-quark interactions are considered. For color confinement potential, the screened form is used,

$$V_{CON}(\mathbf{r}_{ij}) = \boldsymbol{\lambda}_i^c \cdot \boldsymbol{\lambda}_j^c [-a_c(1 - e^{-\mu_c r_{ij}}) + \Delta], \quad (2)$$

where  $a_c$ ,  $\mu_c$  and  $\Delta$  are model parameters, and  $\boldsymbol{\lambda}^c$  represent the SU(3) color Gell-Mann matrices.

One-gluon exchange potential contains so-called coulomb and color-magnetism interactions, which arise from QCD perturbation effects,

$$V_{OGE}(\mathbf{r}_{ij}) = \frac{1}{4} \alpha_s \boldsymbol{\lambda}_i^c \cdot \boldsymbol{\lambda}_j^c \left[ \frac{\boldsymbol{\sigma}_i \cdot \boldsymbol{\sigma}_j}{r_{ij}} - \frac{1}{6m_i m_j} \frac{e^{-r_{ij}/r_0(\mu)}}{r_{ij} r_0^2(\mu)} \right], \quad (3)$$

$\mu$  is the reduced mass between two interacting quarks;  $\boldsymbol{\sigma}$  represent the SU(2) Pauli matrices;  $r_0(\mu) = \hat{r}_0/\mu$ ;  $\alpha_s$  denotes the effective scale-dependent strong running coupling constant of one-gluon exchange,

$$\alpha_s = \frac{\alpha_0}{\ln\left(\frac{\mu^2 + \mu_0^2}{\Lambda_0^2}\right)}. \quad (4)$$

Due to chiral symmetry spontaneous breaking, Goldstone boson exchange potentials appear between light quarks ( $u, d$  and  $s$ ),

$$\begin{aligned} V_{GBE}(\mathbf{r}_{ij}) &= V_\pi(\mathbf{r}_{ij}) + V_K(\mathbf{r}_{ij}) + V_\eta(\mathbf{r}_{ij}) + V_{sc}(\mathbf{r}_{ij}), \\ V_\pi(\mathbf{r}_{ij}) &= \frac{g_{ch}^2}{4\pi} \frac{m_\pi^2}{12m_i m_j} \frac{\Lambda_\pi^2 m_\pi}{\Lambda_\pi^2 - m_\pi^2} [Y(m_\pi r_{ij}) \\ &\quad - \frac{\Lambda_\pi^3}{m_\pi^3} Y(\Lambda_\pi r_{ij})] (\boldsymbol{\sigma}_i \cdot \boldsymbol{\sigma}_j) \sum_{a=1}^3 \lambda_i^a \lambda_j^a, \\ V_K(\mathbf{r}_{ij}) &= \frac{g_{ch}^2}{4\pi} \frac{m_K^2}{12m_i m_j} \frac{\Lambda_K^2 m_K}{\Lambda_K^2 - m_K^2} [Y(m_K r_{ij}) \\ &\quad - \frac{\Lambda_K^3}{m_K^3} Y(\Lambda_K r_{ij})] (\boldsymbol{\sigma}_i \cdot \boldsymbol{\sigma}_j) \sum_{a=4}^7 \lambda_i^a \lambda_j^a, \\ V_\eta(\mathbf{r}_{ij}) &= \frac{g_{ch}^2}{4\pi} \frac{m_\eta^2}{12m_i m_j} \frac{\Lambda_\eta^2 m_\eta}{\Lambda_\eta^2 - m_\eta^2} \\ &\quad [Y(m_\eta r_{ij}) - \frac{\Lambda_\eta^3}{m_\eta^3} Y(\Lambda_\eta r_{ij})] (\boldsymbol{\sigma}_i \cdot \boldsymbol{\sigma}_j) \\ &\quad [\cos \theta_P (\lambda_i^8 \lambda_j^8) - \sin \theta_P (\lambda_i^0 \lambda_j^0)], \end{aligned} \quad (5)$$

$Y(x)$  is the standard Yukawa functions;  $\lambda^a$  are the SU(3) flavor Gell-Mann matrices;  $\Lambda$  are the cut-offs and  $m_\chi$ ,  $\chi = \pi, K, \eta$  are the masses of Goldstone bosons;  $g_{ch}^2$  is the chiral field coupling constant, which is determined from the  $NN\pi$  coupling constant through

$$\frac{g_{ch}^2}{4\pi} = \frac{9}{25} \frac{g_{\pi NN}^2}{4\pi} \frac{m_{u,d}^2}{m_N^2}. \quad (6)$$

Besides, the scalar nonet (the extension of chiral partner  $\sigma$  meson) exchange  $V_{sc}$  is also used in this work, which introduces other higher multi-pion terms that are simulated through the full nonet of scalar mesons exchange

between two constituent quarks [40].

$$\begin{aligned}
V_{sc}(\mathbf{r}_{ij}) &= V_{a_0}(\mathbf{r}_{ij}) \sum_{a=1}^3 \lambda_i^a \lambda_j^a + V_{\kappa}(\mathbf{r}_{ij}) \sum_{a=4}^7 \lambda_i^a \lambda_j^a \\
&+ V_{f_0}(\mathbf{r}_{ij}) \lambda_i^8 \lambda_j^8 + V_{\sigma}(\mathbf{r}_{ij}) \lambda_i^0 \lambda_j^0, \\
V_s(\mathbf{r}_{ij}) &= -\frac{g_{ch}^2}{4\pi} \frac{\Lambda_s^2 m_s}{\Lambda_s^2 - m_s^2} [Y(m_s r_{ij}) - \frac{\Lambda_s}{m_s} Y(\Lambda_s r_{ij})], \\
s &= a_0, \kappa, f_0, \sigma
\end{aligned} \tag{7}$$

The model parameters are listed in Table I, and the calculated baryon and meson masses are presented in the Table II along with the experimental values. Because it is difficult to use the same set of parameters to have a good description of baryon and meson spectra simultaneously, we treat the strong coupling constant of one-gluon exchange with different values for quark-quark and quark-antiquark interacting pairs. From the calculation, most of the results are close to experimental values except for  $\omega$ . In the follow-up calculation, we find that the molecular states consisting of this meson are open channels and these channels have no effect on all stable molecular states so these errors do not affect our final results.

TABLE I: Quark model parameters.

Quark masses	$m_u=m_d$ (MeV)	313
	$m_s$ (MeV)	555
Goldstone bosons	$\Lambda_{\pi}$ (fm $^{-1}$ )	4.20
	$\Lambda_{\eta} = \Lambda_K$ (fm $^{-1}$ )	5.20
	$m_{\pi}$ (fm $^{-1}$ )	0.70
	$m_K$ (fm $^{-1}$ )	2.51
	$m_{\eta}$ (fm $^{-1}$ )	2.77
	$g_{ch}^2/(4\pi)$	0.54
	$\theta_P$ (°)	-15
Confinement	$a_c$ (MeV)	465.3
	$\mu_c$ (fm $^{-1}$ )	0.58
	$\Delta$ (MeV)	164.52
scalar nonet	$m_{\sigma}$ (fm $^{-1}$ )	3.42
	$\Lambda_{\sigma}$ (fm $^{-1}$ )	4.20
	$\Lambda_{a_0} = \Lambda_{\kappa} = \Lambda_{f_0}$ (fm $^{-1}$ )	5.20
	$m_{a_0} = m_{\kappa} = m_{f_0}$ (fm $^{-1}$ )	4.97
OGE	$\hat{r}_0$ (MeV fm)	35.19
	$\alpha_{uu}$	0.467/0.662
	$\alpha_{us}$	0.695/0.573
	$\alpha_{ss}$	0.29/0.335

In the following, the wave functions for the pentaquark systems are constructed and the eigen-energy is obtained by solving the Schrödinger equation. The wave function of the system consists of four parts: orbital, spin, flavor and color. The wave function of each part is constructed in two steps, first construct the wave function of three-quark cluster and quark-antiquark cluster, respectively, then coupling two clusters wave functions to

TABLE II: The masses of ground-state baryons and mesons (unit: MeV).

	$\Lambda$	$\Sigma$	$\Sigma^*$	$\Xi$	$\Xi^*$	$\Omega$
CHQM	1115	1191	1392	1318	1537	1672
Expt	1116	1189	1386	1315	1530	1672
	$\pi$	$\rho$	$\bar{K}$	$\bar{K}^*$	$\eta'$	$\phi$
CHQM	139	768	498	915	958	1048
Expt	140	775	498	892	958	1020
	$\eta$	$\omega$				
CHQM	560	590				
Expt	548	782				

form the complete five-body one. In this work, the wave functions for  $(ssq)(\bar{q}s)$  configuration is written down, the wave functions for other configuration can be obtained by exchange the indices of particles. The indices of particles  $s, s, q, \bar{q}, s$  are 1,2,3,4,5. As an example the wave functions for  $(sss)(\bar{q}q)$  are obtained by exchange the particle indices  $3 \leftrightarrow 5$ .

The first part is orbital wave function. A five-body system have four relative motions so it is written as follows.

$$\psi_{LM_L}^x = [ [ [\psi_{n_1 l_1}(\boldsymbol{\rho}) \psi_{n_2 l_2}(\boldsymbol{\lambda})]_l \psi_{n_3 l_3}(\mathbf{r}) ]_{l'} \psi_{n_4 l_4}(\mathbf{R}) ]_{LM_L}, \tag{8}$$

where the Jacobi coordinates are defined as follows,

$$\begin{aligned}
\boldsymbol{\rho} &= \mathbf{x}_1 - \mathbf{x}_2, \\
\boldsymbol{\lambda} &= \left( \frac{m_1 \mathbf{x}_1 + m_2 \mathbf{x}_2}{m_1 + m_2} \right) - \mathbf{x}_3, \\
\mathbf{r} &= \mathbf{x}_4 - \mathbf{x}_5, \\
\mathbf{R} &= \left( \frac{m_1 \mathbf{x}_1 + m_2 \mathbf{x}_2 + m_3 \mathbf{x}_3}{m_1 + m_2 + m_3} \right) - \left( \frac{m_4 \mathbf{x}_4 + m_5 \mathbf{x}_5}{m_4 + m_5} \right).
\end{aligned} \tag{9}$$

$\mathbf{x}_i$  is the position of the  $i$ -th particle. Then we use a set of gaussians to expand the radial part of the orbital wave function which is shown below,

$$\psi_{lm}(\mathbf{r}) = \sum_{n=1}^{n_{max}} c_{nl} \phi_{nlm}^G(\mathbf{r}) \tag{10}$$

$$\phi_{nlm}^G(\mathbf{r}) = N_{nl} r^l e^{-\nu_n r^2} Y_{lm}(\hat{\mathbf{r}}) \tag{11}$$

where  $N_{nl}$  is the normalization constant,

$$N_{nl} = \left( \frac{2^{l+2} (2\nu_n)^{l+3/2}}{\sqrt{\pi} (2l+1)!!} \right)^{\frac{1}{2}}, \tag{12}$$

and  $c_{nl}$  is the variational parameter, which is determined by the dynamics of the system. The Gaussian size parameters are chosen according to the following geometric progression:

$$\nu_n = \frac{1}{r_n^2}, r_n = r_{min} a^{n-1}, a = \left( \frac{r_{max}}{r_{min}} \right)^{\frac{1}{n_{max}-1}}, \tag{13}$$

where  $n_{max}$  is the number of Gaussian functions, and  $n_{max}$  is determined by the convergence of the results. In the present calculation,  $n_{max} = 8$  and the results of calculation tends to be stable.

The details of constructing flavor, color and spin wave functions of 5-quark system can be found in Ref. [32], and only the last expressions are shown here.

For flavor wave functions, two possible quantum numbers  $I = 0$  and  $I = 1$  in two configurations are considered:

$$\begin{aligned}
|\chi_{0,0}^{f1}\rangle &= \frac{1}{\sqrt{2}}(ssu\bar{d}s - ssd\bar{d}s) \\
|\chi_{0,0}^{f2}\rangle &= -\frac{1}{\sqrt{2}}(sss\bar{u}u + sss\bar{d}d) \\
|\chi_{1,1}^{f3}\rangle &= ssu\bar{d}s \\
|\chi_{1,1}^{f4}\rangle &= sss\bar{d}u
\end{aligned} \tag{14}$$

Color wave functions:

$$\begin{aligned}
|\chi^{c1}\rangle &= \frac{1}{\sqrt{18}}(rgb - rbg + gbr - grb + brg - bgr) \\
&\quad (\bar{r}r + \bar{g}g + \bar{b}b) \\
|\chi^{c2}\rangle &= \frac{1}{\sqrt{192}} [2(2rrg - rgr - grr)\bar{r}b \\
&\quad + 2(rgg + grg - 2ggr)\bar{g}b \\
&\quad - 2(2rrb - rbr - brr)\bar{r}g - 2(rbb + brb - 2bbr)\bar{b}g \\
&\quad + 2(2ggb - gbg - bgg)\bar{g}r + 2(gbb + bgb - 2bbg)\bar{b}r \\
&\quad + (rbg - gbr + brg - bgr)(2\bar{b}b - \bar{r}r - \bar{g}g) \\
&\quad + (2rgb - rgb + 2grb - gbr - brg - bgr)(\bar{r}r - \bar{g}g)] \\
|\chi^{c3}\rangle &= \frac{1}{24} [6(rgg - grr)\bar{r}b + 6(rgg - grg)\bar{g}b \\
&\quad - 6(rbr - brr)\bar{r}g - 6(rbb - brb)\bar{b}g \\
&\quad + 6(gbg - bgg)\bar{g}r + 6(gbb - bgb)\bar{b}r \\
&\quad + 3(rbg + gbr - brg - bgr)(\bar{r}r - \bar{g}g) \\
&\quad + (2rgb + rgb - 2grb - gbr - brg + bgr) \\
&\quad (2\bar{b}b - \bar{r}r - \bar{g}g)]
\end{aligned} \tag{15}$$

Spin wave functions:

$$\begin{aligned}
|\chi_{\frac{1}{2},\frac{1}{2}}^{\sigma 1}\rangle &= \frac{1}{\sqrt{12}}(2\alpha\alpha\beta\alpha\beta - 2\alpha\alpha\beta\beta\alpha + \alpha\beta\alpha\beta\alpha \\
&\quad - \alpha\beta\alpha\alpha\beta + \beta\alpha\alpha\beta\alpha - \beta\alpha\alpha\alpha\beta) \\
|\chi_{\frac{1}{2},\frac{1}{2}}^{\sigma 2}\rangle &= \frac{1}{2}(\alpha\beta\alpha\alpha\beta - \alpha\beta\alpha\beta\alpha + \beta\alpha\alpha\beta\alpha - \beta\alpha\alpha\alpha\beta) \\
|\chi_{\frac{1}{2},\frac{1}{2}}^{\sigma 3}\rangle &= \frac{1}{6}(2\alpha\alpha\beta\alpha\beta + 2\alpha\alpha\beta\beta\alpha - \alpha\beta\alpha\alpha\beta - \alpha\beta\alpha\beta\alpha \\
&\quad - \beta\alpha\alpha\beta\alpha - \beta\alpha\alpha\alpha\beta - 2\alpha\beta\beta\beta\alpha - 2\beta\alpha\beta\alpha\alpha \\
&\quad + 4\beta\beta\alpha\alpha\alpha) \\
|\chi_{\frac{1}{2},\frac{1}{2}}^{\sigma 4}\rangle &= \frac{1}{\sqrt{12}}(\alpha\beta\alpha\alpha\beta + \alpha\beta\alpha\beta\alpha - \beta\alpha\alpha\alpha\beta - \beta\alpha\alpha\beta\alpha \\
&\quad + 2\beta\alpha\beta\alpha\alpha - 2\alpha\beta\beta\beta\alpha)
\end{aligned} \tag{16}$$

$$\begin{aligned}
|\chi_{\frac{1}{2},\frac{1}{2}}^{\sigma 5}\rangle &= \frac{1}{\sqrt{18}}(3\alpha\alpha\alpha\beta\beta - \alpha\alpha\beta\alpha\beta - \alpha\alpha\beta\beta\alpha \\
&\quad - \alpha\beta\alpha\alpha\beta - \alpha\beta\alpha\beta\alpha - \beta\alpha\alpha\alpha\beta - \beta\alpha\alpha\beta\alpha \\
&\quad + \beta\beta\alpha\alpha\alpha + \beta\alpha\beta\alpha\alpha + \alpha\beta\beta\alpha\alpha) \\
|\chi_{\frac{3}{2},\frac{3}{2}}^{\sigma 6}\rangle &= \frac{1}{\sqrt{6}}(2\alpha\alpha\beta\alpha\alpha - \alpha\beta\alpha\alpha\alpha - \beta\alpha\alpha\alpha\alpha) \\
|\chi_{\frac{3}{2},\frac{3}{2}}^{\sigma 7}\rangle &= \frac{1}{\sqrt{2}}(\alpha\beta\alpha\alpha\alpha - \beta\alpha\alpha\alpha\alpha) \\
|\chi_{\frac{3}{2},\frac{3}{2}}^{\sigma 8}\rangle &= \frac{1}{\sqrt{2}}(\alpha\alpha\alpha\alpha\beta - \alpha\alpha\alpha\beta\alpha) \\
|\chi_{\frac{3}{2},\frac{3}{2}}^{\sigma 9}\rangle &= \frac{1}{\sqrt{30}}(2\alpha\alpha\beta\alpha\alpha + 2\alpha\beta\alpha\alpha\alpha + 2\beta\alpha\alpha\alpha\alpha \\
&\quad - 3\alpha\alpha\alpha\alpha\beta - 3\alpha\alpha\alpha\beta\alpha) \\
|\chi_{\frac{5}{2},\frac{5}{2}}^{\sigma 10}\rangle &= \alpha\alpha\alpha\alpha\alpha,
\end{aligned}$$

where  $\chi^{c1}$  represents the color wave function of a color singlet-singlet structure,  $\chi^{c2}$  and  $\chi^{c3}$  represent the color octet-octet wave functions respectively. The subscripts of  $\chi_{I,I_z}^f$  ( $\chi_{S,S_z}^\sigma$ ) are total isospin (spin) and its third projection.

Finally, the total wave function of the five-quark system is written as:

$$\Psi_{JM_J}^{i,j,k} = \mathcal{A} \left[ [\psi_L \chi_S^\sigma]_{JM_J} \chi_j^{f_i} \chi_k^{c_i} \right], \tag{17}$$

where the  $\mathcal{A}$  is the antisymmetry operator of the system which guarantees the antisymmetry of the total wave functions when identical particles exchange. Under our numbering scheme, the antisymmetry operator has the following form,

$$\mathcal{A} = 1 - (15) - (25).$$

At last, we solve the following Schrödinger equation to obtain eigen-energies of the system,

$$H\Psi_{JM_J} = E\Psi_{JM_J}, \tag{18}$$

with the help of the Rayleigh-Ritz variational principle. The matrix elements of Hamiltonian can be easily obtained if all the orbital angular momenta are zero, which is reasonable for only considering the low-lying states of pentaquark systems. It is worthwhile to mention that if the orbital angular momenta of the systems are not zero, it is necessary to use the infinitesimally shifted Gaussian method to calculate the matrix elements [31].

### III. RESULTS AND DISCUSSIONS

In this section, we present the results of possible  $S$ -wave of pentaquark systems  $ssq\bar{q}s$ ,  $q = u, d$  with all possible quantum numbers  $IJ^P = 0(\frac{1}{2})^-$ ,  $0(\frac{3}{2})^-$ ,  $0(\frac{5}{2})^-$ ,  $1(\frac{1}{2})^-$ ,  $1(\frac{3}{2})^-$  and  $1(\frac{5}{2})^-$ . All the orbital angular momentum of the systems are treated as zero and the corresponding parity is negative.

TABLE III: The results for system with  $IJ^P = 0\frac{1}{2}^-$ . cc1: mixing of color singlet-singlet channels, cc2: mixing of all channels. (unit: MeV)

$\psi^{fi}$	$\psi^{\sigma j}$	$\psi^{ck}$	Channel	E	$E_{th}^{Theo}$	$E_B$	$E_{th}^{Exp}$	$E'$
$i = 1$	$j = 1$	$k = 1$	$\Xi\bar{K}$	1816	1816	0	1813	1813
$i = 1$	$j = 1, 2$	$k = 1, 2, 3$		1816				
$i = 1$	$j = 3$	$k = 1$	$\Xi\bar{K}^*$	2178	2232	-54	2207	2153
$i = 1$	$j = 3, 4$	$k = 1, 2, 3$		2166		-66		2141
$i = 1$	$j = 5$	$k = 1$	$\Xi^*\bar{K}^*$	2438	2451	-13	2422	2409
$i = 1$	$j = 5$	$k = 1, 3$		2430		-21		2401
$i = 2$	$j = 5$	$k = 1$	$\Omega\omega$	2261	2262	0	0	2454
$i = 2$	$j = 5$	$k = 1, 3$		2261				
cc1					1816	0		
cc2					1816			

TABLE IV: The results for system with  $IJ^P = 1\frac{1}{2}^-$ . cc1: mixing of color singlet-singlet channels, cc2: mixing of all channels. (unit: MeV)

$\psi^{fi}$	$\psi^{\sigma j}$	$\psi^{ck}$	Channel	E	$E_{th}^{Theo}$	$E_B$	$E_{th}^{Exp}$	$E'$
$i = 3$	$j = 1$	$k = 1$	$\Xi\bar{K}$	1816	1816	0	1813	1813
$i = 3$	$j = 1, 2$	$k = 1, 2, 3$		1816				
$i = 3$	$j = 3$	$k = 1$	$\Xi\bar{K}^*$	2220	2232	-12	2207	2195
$i = 3$	$j = 3, 4$	$k = 1, 2, 3$		2208		-24		2283
$i = 3$	$j = 5$	$k = 1$	$\Xi^*\bar{K}^*$	2431	2451	-20	2422	2402
$i = 3$	$j = 5$	$k = 1, 3$		2420		-31		2391
$i = 4$	$j = 5$	$k = 1$	$\Omega\rho$	2440	2440	0	0	2447
$i = 4$	$j = 5$	$k = 1, 3$		2440				
cc1					1816	0		
cc2					1816			

In Tables III-VIII, the significant calculation results are shown. In each table, columns 1 to 3 represent the indices of flavor, spin and color wave functions in each channel. Column 4 is the corresponding physical channel of pentaquark systems. In column 5, the eigen-energy of each channel is listed and the theoretical threshold (the sum of the theoretical masses of corresponding baryon and meson) is given in column 6. Column 8 gives the binding energies, which are the difference between the eigen-energy and the theoretical threshold. Finally, the experimental thresholds (the sum of the experimental masses of the corresponding baryon and meson) along with corrected energies (the sum of experimental threshold and the binding energy,  $E' = E_B + E_{th}^{exp}$ ) are given in last two columns. With this correction, the calculation error caused by the model parameters in pentaquark calculation can be reduced partly. The results are analyzed in the following.

(a)  $IJ^P = 0\frac{1}{2}^-$  (Table III): Single-color structure calculation shows that there exist two bound states in  $\Xi\bar{K}^*$  and  $\Xi^*\bar{K}^*$  channels while  $\Xi\bar{K}$  and  $\Omega\eta$  are unbound. After coupling to respective hidden-color channels, the binding energy of two bound states increase by a few MeVs. When coupled-channel calculation between both single-

color structure and all type of structure is performed, the lowest energy is above the threshold of  $\Xi\bar{K}$ . So no bound state can be formed in  $IJ^P = 0\frac{1}{2}^-$  system. However, resonances are possible because the strong attractions exist both in  $\Xi\bar{K}^*$  and  $\Xi^*\bar{K}^*$  channels. Thus, real-scaling method is required to identify resonances.

(b)  $IJ^P = 1\frac{1}{2}^-$  (Table IV): The results are similar to that of  $IJ^P = 0\frac{1}{2}^-$  system, there are bound states in  $\Xi\bar{K}^*$  and  $\Xi^*\bar{K}^*$  channels and other two channels are unbound. The lowest eigen-energy of channel coupling calculation is above the threshold of  $\Xi\bar{K}$ , so no bound state found in  $IJ^P = 1\frac{1}{2}^-$  system.  $\Xi\bar{K}^*$  and  $\Xi^*\bar{K}^*$  are possible resonances.

(c)  $IJ^P = 0\frac{3}{2}^-$  (Table V): The single channel calculations show that there exists bound state in  $\Xi^*\bar{K}^*$  channel. Moreover, the attraction increases after coupling to its hidden-color channel. Although the single channel calculation shows that the state  $\Xi^*\bar{K}$  is unbound, the couple-channels calculations push the states below the threshold. The coupling of all color singlet-singlet channels find the lowest eigen-energy of the system is 2029 MeV, 6 MeV below the threshold, The full channel coupling lower the lowest eigen-energy to 2025 MeV. So a

TABLE V: The results for system with  $IJ^P = 0\frac{3}{2}^-$ . cc1: mixing of color singlet-singlet channels, cc2: mixing of all channels. (unit: MeV)

$\psi^{fi}$	$\psi^{\sigma j}$	$\psi^{ck}$	Channel	E	$E_{th}^{Theo}$	$E_B$	$E_{th}^{Exp}$	$E'$
$i = 1$	$j = 6$	$k = 1$	$\Xi \bar{K}^*$	2232	2232	0	2207	2207
$i = 1$	$j = 6, 7$	$k = 1, 2, 3$		2232				
$i = 1$	$j = 8$	$k = 1$	$\Xi^* \bar{K}$	2035	2035	0	2028	2028
$i = 1$	$j = 8$	$k = 1, 3$		2035				
$i = 1$	$j = 9$	$k = 1$	$\Xi^* \bar{K}^*$	2413	2451	-38	2422	2384
$i = 1$	$j = 9$	$k = 1, 3$		2378		-73		2349
$i = 2$	$j = 8$	$k = 1$	$\Omega \eta$	2232	2232	0	0	2220
$i = 2$	$j = 8$	$k = 1, 3$		2232				
$i = 2$	$j = 9$	$k = 1$	$\Omega \omega$	2262	2262	0	0	2454
$i = 2$	$j = 9$	$k = 1, 3$		2262				
cc1					2029	-6		
cc2					2025	-10		

TABLE VI: The results for system with  $IJ^P = 1\frac{3}{2}^-$ . cc1: mixing of color singlet-singlet channels, cc2: mixing of all channels. (unit: MeV)

$\psi^{fi}$	$\psi^{\sigma j}$	$\psi^{ck}$	Channel	E	$E_{th}^{Theo}$	$E_B$	$E_{th}^{Exp}$	$E'$
$i = 3$	$j = 6$	$k = 1$	$\Xi \bar{K}^*$	2232	2232	0	2207	2207
$i = 3$	$j = 6, 7$	$k = 1, 2, 3$		2232				
$i = 3$	$j = 8$	$k = 1$	$\Xi^* \bar{K}$	2035	2035	0	2028	2028
$i = 3$	$j = 8$	$k = 1, 3$		2035				
$i = 3$	$j = 9$	$k = 1$	$\Xi^* \bar{K}^*$	2444	2451	-7	2422	2415
$i = 3$	$j = 9$	$k = 1, 3$		2436		-15		2407
$i = 4$	$j = 8$	$k = 1$	$\Omega \pi$	1811	1811	0	1812	1812
$i = 4$	$j = 8$	$k = 1, 3$		1811				
$i = 4$	$j = 9$	$k = 1$	$\Omega \rho$	2440	2440	0	0	2447
$i = 4$	$j = 9$	$k = 1, 3$		2440				
cc1					1810	-1		
cc2					1809	-2		

bound state (main component is  $\Xi^* \bar{K}$ ) can be formed after the channel coupling in  $IJ^P = 0\frac{3}{2}^-$  system, which is regarded as a good candidate for  $\Omega(2012)$ . Also, it is possible for  $\Xi^* \bar{K}^*$  to form a resonance.

(d)  $IJ^P = 1\frac{3}{2}^-$  (Table VI): The results are again similar to that of  $IJ^P = 0\frac{3}{2}^-$  system. There is only one bound state,  $\Xi^* \bar{K}^*$  in the single channel calculation, and it is possible to become a resonance. In addition, the channel coupling leads to a bound state in the system. the lowest eigen-energy is 1810 MeV (color singlet-singlet channel coupling), or 1809 MeV (full channel coupling), 1 MeV or 2 MeV lower than the threshold of the lowest channel  $\Omega \pi$ . So there is a bound state for the  $IJ^P = 1\frac{3}{2}^-$  system.

(e) For  $J^P = \frac{5}{2}^-, I = 0, 1$  (Table VII and (Table VIII): The results of these two systems are similar. There is no bound state and the conclusions are the same after full-channel coupling.

From the above results, one can that the iso-scalar and iso-vector states have similar behavior, generally the iso-vector states have a little higher energy than that of the corresponding iso-scalar states. This fact infers that the state are molecular one, the large separation between baryon and meson minimize the contribution from the pion exchange potential. In the following, we shall calculation the separations between quarks to verify the molecule picture of the state.

We make a comparison between our calculation results and that of Ref. [30]. The binding energies of states obtained in our work are generally bigger, basically on the order of tens since we consider the effects of scalar nonet exchange, whose contributions are strongly attractive to bind two hadrons together in our work, in Ref. [30], only  $\sigma$ -exchange between non-strange quarks is considered. For example, the binding energy of  $[\Xi \bar{K}^*]_{0\frac{1}{2}^-}$  is 54 MeV, whereas it is 8 MeV in Ref. [30]. And it is reasonable that  $[\Xi^* \bar{K}^*]_{0\frac{1}{2}^-}$ ,  $[\Xi \bar{K}^*]_{1\frac{1}{2}^-}$  and  $[\Xi^* \bar{K}^*]_{1\frac{1}{2}^-}$  with

TABLE VII: The results for system with  $IJ^P = 0\frac{5}{2}^-$ . cc1: mixing of color singlet-singlet channels, cc2: mixing of all channels. (unit: MeV)

$\psi^{fi}$	$\psi^{\sigma j}$	$\psi^{ck}$	Channel	E	$E_{th}^{Theo}$	$E_B$	$E_{th}^{Exp}$	$E'$
$i = 1$	$j = 10$	$k = 1$	$\Xi^* \bar{K}^*$	2451	2451	0	2422	2422
$i = 1$	$j = 10$	$k = 1, 3$		2451				
$i = 2$	$j = 10$	$k = 1$	$\Omega\omega$	2262	2262	0	2454	2454
$i = 2$	$j = 10$	$k = 1, 3$		2262				
cc1					2262	0		
cc2					2262			

TABLE VIII: The results for system with  $IJ^P = 1\frac{5}{2}^-$ . cc1: mixing of color singlet-singlet channels, cc2: mixing of all channels. (unit: MeV)

$\psi^{fi}$	$\psi^{\sigma j}$	$\psi^{ck}$	Channel	E	$E_{th}^{Theo}$	$E_B$	$E_{th}^{Exp}$	$E'$
$i = 3$	$j = 10$	$k = 1$	$\Xi^* \bar{K}^*$	2451	2451	0	2422	2422
$i = 3$	$j = 10$	$k = 1, 3$		2447				
$i = 4$	$j = 10$	$k = 1$	$\Omega\rho$	2440	2440	0	2447	2447
$i = 4$	$j = 10$	$k = 1, 3$		2440				
cc1					2440	0		
cc2					2440			

more than a dozen of binding energies in our work and they become unbound in Ref. [30]. For  $IJ^P = 0\frac{3}{2}^-$  system, we solve the mass inversion problem of  $\Xi^* \bar{K}$  and  $\Omega\eta$ , which leads to a more objective description on the effect of channel-coupling. Then, come to  $IJ^P = 1\frac{3}{2}^-$  system, there is no mass inversion problem in both two calculations, we found that our results are consistent with that of Ref. [30]. Finally, for  $IJ^P = 0\frac{5}{2}^-$  and  $1\frac{5}{2}^-$  systems, the results are the same in both two calculations, there is no any bound state.

To check whether the resonances in  $IJ^P = 0\frac{1}{2}^-$ ,  $0\frac{3}{2}^-$ ,  $1\frac{3}{2}^-$  and  $1\frac{3}{2}^-$  systems can survive after coupling to the open channels, a stability method to identify genuine resonance states, real-scaling method (stabilization method) [36–38], is employed. In this method, the Gaussian size parameter  $r_n$ , appearing in Eq. (13), for the basis functions between the color-singlet baryon and meson clusters is scaled by a factor  $\alpha$ :  $r_n \rightarrow \alpha r_n$ . As a result, a genuine resonance will act as an avoid-crossing structure (see Fig. 1) with the increasing of  $\alpha$ , while other continuum states will fall off towards its threshold. If the avoid-crossing structure is repeated periodically as  $\alpha$  increase, then the avoid-crossing structure is a genuine resonance.

Our results are shown in Figs. 2, 3, 4 and 5. In these figures, the thresholds of all physical channels appear as horizontal lines and are marked with lines (red lines), along with their contents tagged. And for genuine resonances, which appear as avoid-crossing structure and are marked with blue lines. Bound states are also marked with blue line below the lowest threshold of the systems. The continuum states fall off towards their respective

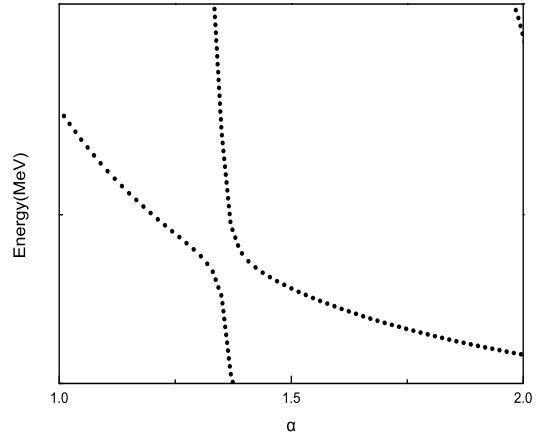
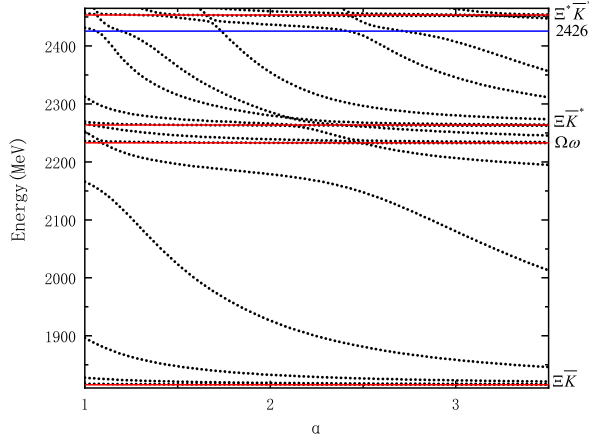
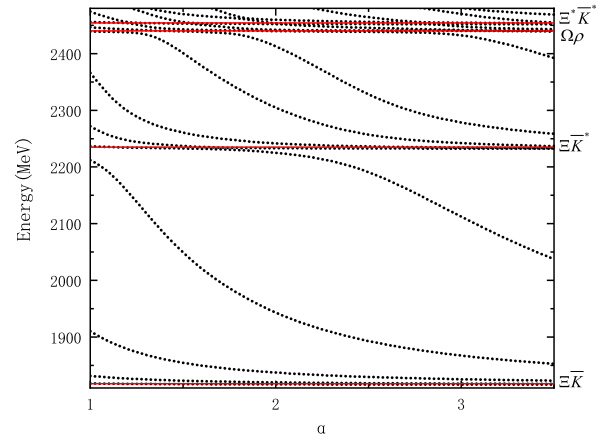
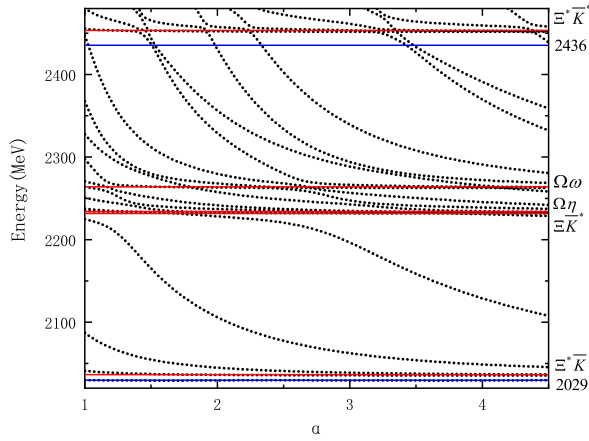
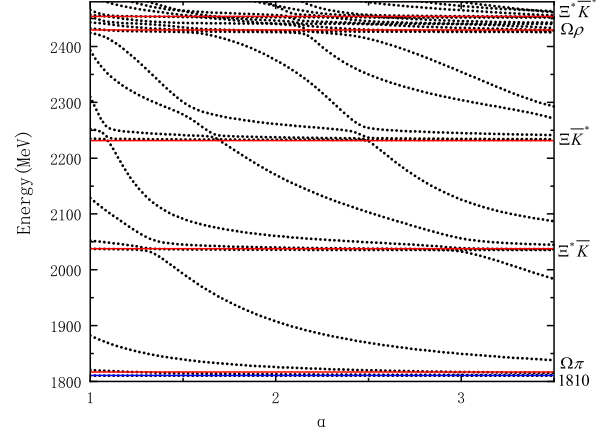


FIG. 1: The shape of the resonance in real-scaling method

threshold (red horizontal lines). For  $IJ^P = 0\frac{5}{2}^-, 1\frac{5}{2}^-$  systems, since there is no any bound state in single-channel calculations, which means no mechanism of forming resonances, we do not present the results of these two systems.

For  $IJ^P = 0\frac{1}{2}^-$  system, we get one resonance whose energy is 2426 MeV (main component is  $\Xi^* \bar{K}^*$ ). The other possible resonance,  $\Xi \bar{K}^*$ , decays strongly to the open channels and cannot form an avoid-crossing structure, so we do not think it is a observable resonance. In  $IJ^P = 0\frac{3}{2}^-$  system, there is only one resonance and

FIG. 2: Energy spectrum of  $0\frac{1}{2}^-$  system.FIG. 4: Energy spectrum of  $1\frac{1}{2}^-$  system.FIG. 3: Energy spectrum of  $0\frac{3}{2}^-$  system.FIG. 5: Energy spectrum of  $1\frac{3}{2}^-$  system.

its energy is 2436 MeV (main component is  $\Xi^* \bar{K}^*$ ), and there is also a bound state which lies below the lowest threshold (a blue line marked by 2029). Although there are two channels where exist weakly bound states in the single channel calculation for the  $IJ^P = 1\frac{1}{2}^-$  system, we found no avoid-crossing structure, which means there is no any resonance. Finally, in  $IJ^P = 1\frac{3}{2}^-$  system, there is no any resonance. However, the lowest energy of this system is pushed below the lowest threshold of the system  $\Omega\pi$  by the channel coupling, thus there is a bound states which is shown as a blue line marked by 1810. It is worth mentioning that in case we use real-scaling method to identify resonances, we will also calculate the composition of the possible resonances to find the mechanism of the formation of the resonances. The main component of a genuine resonance should be bound state chan-

nels in the single channel calculation or coupled channels with energy below the the lowest threshold of the coupling channels in the channel coupling calculation. For example, in Fig. 5, there is an avoid-crossing structure around 2250 MeV. However, its main component is  $\Omega\omega$ , a open channel, which means the avoid-crossing structure is formed by two or more open channels which have different falling slopes.

For resonances, the partial widths of two hadrons strong decay can be extracted from these figures. The decay width of resonance to possible open channels of two hadrons is obtained by the following formula

$$\Gamma = 4V(\alpha) \frac{\sqrt{k_r k_c}}{|k_r - k_c|}, \quad (19)$$

where  $V(\alpha)$  is the minimum energy difference, while  $k_c$

TABLE IX: The decay width and RSM distances of  $\Omega$  states in all systems.

Model	$IJ^P$	State	Main comp.	$E'$	Width	$r_{12}$	$r_{13}$	$r_{14}$	$r_{15}$	$r_{34}$	$r_{35}$	$r_{45}$
Resonance	$0\frac{1}{2}^-$	$\Omega(2426)$	$\Xi^* \bar{K}^*$	2396	73.5	0.7	0.9	1.5	1.6	1.6	1.6	0.9
	$0\frac{3}{2}^-$	$\Omega(2436)$	$\Xi^* \bar{K}^*$	2417	68.4	0.5	0.9	2.1	2.2	2.2	2.1	0.8
Bound state	$0\frac{3}{2}^-$	$\Omega(2029)$	$\Xi^* \bar{K}$	2018	-	0.7	0.8	2.3	2.3	2.3	2.3	0.5
	$1\frac{3}{2}^-$	$\Omega(1809)$	$\Omega\pi$	1810	-	0.7	0.7	3.5	3.5	3.5	3.5	0.5

and  $k_r$  stand for the slopes of scattering state and resonance state respectively. More details can be found in Ref. [36]. And the total widths also include the decay width of each hadron in the pentaquark state. For bound states, they have no widths due to their stability against the strong decay. After a series of calculations and identification, we also calculate the root-mean-square (RMS) distances between any two quarks in all bound states and observable resonances to determine their inner structure respectively and the results are shown in Table IX. The main component of each resonance and corrected energy are also given.

From Table IX, we can see that, for two resonances  $\Omega(2426)$  and  $\Omega(2436)$ , the decay widths are 73.5 MeV and 68.4 MeV respectively. The distances among quarks 1, 2 and 3 are 0.5-0.9 fm and the distances between quark 4 and anti-quark are 0.8-0.9 fm, while the distances between quarks 1, 2, 3 and 4, 5 are over 1.5 fm. Thus it is natural to describe these two resonances as molecular states. In addition, the distance of  $\Omega(2426)$  between two clusters is obviously lower than that of  $\Omega(2436)$  due to its higher binding energy of main component channel  $\Xi^* \bar{K}^*$ . For  $\Omega(2029)$ , the distances between quarks shows its structure is molecular state. Also, the binding energy of the state in single channel is 6 MeV and after coupling to hidden-color channels, the binding energy increase by a few MeVs, which is the typical range of binding energy of hadronic molecules. The corrected energy of molecular state  $\Omega(2029)$  is 2018 MeV, closed to 2012 MeV, so it is a good candidate for  $\Omega(2012)$  reported by Belle collaboration. Nevertheless, in present work, we only consider all possible low-lying states of pentaquark systems with all orbital angular momentum set to 0. Release this constraint, the state  $\Omega(2029)$  can decay to  $D$ -waves  $\Xi \bar{K}$  via the tensor interaction. So considering the effect of all possible  $D$ -wave channels is our further study. For  $\Omega(1809)$ , its result is similar to  $\Omega(2029)$  and the structure of the

state is molecular one. However, the very small binding energy and the distance between two clusters of  $\Omega(1809)$  is over 3 fm, which means it is a loose bound state.

#### IV. SUMMARY

In this work, all low-lying states of  $sssqq, q = u, d$  pentaquark systems are systematically investigated by means of the real scaling method in the framework of chiral quark model, with the help of a high-precision numerical approach, Gaussian expansion method.

The results show that  $\Omega(2012)$  reported by Belle Collaboration can be described as  $\Xi^* \bar{K}$  molecular state with  $IJ^P = 0\frac{3}{2}^-$ . In addition, a very loose bound state  $\Omega(1810)$  with  $IJ^P = 1\frac{3}{2}^-$  and two observable resonances,  $\Omega(2396)$ ,  $\Omega(2417)$  with  $IJ^P = 0\frac{1}{2}^-, 0\frac{3}{2}^-$  are found. The root-mean-square (RMS) distances between any two quarks of these states are also calculated to determine their structures, along with their decay widths. The results shows that four stable states are all molecular states. We hope the states proposed above can be searched in future experiments. Nevertheless, we cannot ignore the mixing of  $S$ - and  $D$ -wave of all states when the spin-orbit and tensor interactions are considered. So further study is expected.

#### Acknowledgments

The work is supported partly by the National Natural Science Foundation of China under Grant Nos. 11775118, and 11535005 and Postgraduate Research and Practice Innovation Program of Jiangsu Province under Grant No. KYCX22\_1542.

- 
- |   |  |
|---|--|
| <p>[1] J. Yelton et al. (Belle Collaboration), Phys. Rev. Lett. 121, 052003 (2018).</p> <p>[2] M. Gell-Mann, Phys. Rev. 125, 1067 (1962).</p> <p>[3] Y. Ne'eman, Nucl. Phys. 26, 222 (1961).</p> <p>[4] N. Isgur and G. Karl, Phys. Rev. D 18, 4187 (1978).</p> <p>[5] S. Capstick and N. Isgur, Phys. Rev. D 34, 2809 (1986); AIP Conf. Proc. 132, 267 (1985).</p> <p>[6] Y. Oh, Phys. Rev. D 75, 074002 (2007).</p> | <p>[7] G. P. Engel et al. (BGR Collaboration), Phys. Rev. D 87, 074504 (2013).</p> <p>[8] J.L. Goity, C. Schat, N.N. Scoccola, Phys. Lett. B 564, 83 (2003).</p> <p>[9] L. Y. Xiao and X. H. Zhong, Phys. Rev. D 98, 034004 (2018).</p> <p>[10] T. M. Aliev, K. Azizi, Y. Sarac, and H. Sundu, Phys. Rev. D 98, 014031 (2018).</p> |
|---|--|

- [11] Z.Y. Wang, L.C. Gui, Q.F. Lü, L.Y. Xiao, and X.H. Zhong, *Phys. Rev. D* 98, 114023 (2018).
- [12] E. E. Kolomeitsev and M. F. M. Lutz, *Phys. Lett. B* 585, 243 (2004).
- [13] S. Sarkar, E. Oset, and M. J. Vicente Vacas, *Nucl. Phys. A* 750, 294 (2005); 780, 90(E) (2006).
- [14] S.G. Yuan, C.S. An, K.W. Wei, B.S. Zou, and H.S. Xu, *Phys. Rev. C* 87 (2013) 025205.
- [15] S.Q. Xu, J.J. Xie, X.R. Chen, and D.J. Jia, *Commun. Theor. Phys.* 65, 53 (2016).
- [16] M.V. Polyakov, H.D. Son, B.D. Sun, A. Tandogan, *Phys. Lett. B* 792, 315 (2019).
- [17] F.K. Guo, C. Hanhart, U.G. Meissner, Q. Wang, Q. Zhao, B.S. Zou, *Rev. Mod. Phys.* 90, 015004 (2018).
- [18] M. P. Valderrama, *Phys. Rev. D* 98, 054009 (2018).
- [19] R. Pavao and E. Oset, *Eur. Phys. J. C* 78, 857 (2018).
- [20] Y. H. Lin and B. S. Zou, *Phys. Rev. D* 98, 056013 (2018).
- [21] Y. Huang, M. Z. Liu, J. X. Lu, J. J. Xie, and L. S. Geng, *Phys. Rev. D* 98, 076012 (2018).
- [22] S. Jia et al. [Belle Collaboration], *Phys. Rev. D* 100, 032006 (2019).
- [23] N. Ikeno, G. Toledo, and E. Oset, *Phys. Rev. D* 101, 094016 (2020).
- [24] J. X. Lu, C. H. Zeng, E. Wang, J. J. Xie, and L. S. Geng, *Eur. Phys. J. C* 80, 361 (2020).
- [25] Y. H. Lin, F. Wang, and B. S. Zou, *Phys. Rev. D* 102, 074025 (2020).
- [26] T. Gutsche and V. E. Lyubovitskij, *J. Phys. G* 48, 025001 (2020)
- [27] M. S. Liu, K. L. Wang, Q. F. Lu, and X. H. Zhong, *Phys. Rev. D* 101, 016002 (2020).
- [28] C. H. Zeng, J. X. Lu, E. Wang, J. J. Xie, and L. S. Geng, *Phys. Rev. D* 102, 076009 (2020).
- [29] (Belle Collaboration), [arXiv:2207.03090 [hep-ex]].
- [30] X. J. Liu, H. X. Huang, J. L. Ping, and D. Y. Chen, *Phys. Rev. C* 103, 025202 (2021).
- [31] E. Hiyama, Y. Kino, and M. Kamimura, *Prog. Part. Nucl. Phys.* 51, 223 (2003).
- [32] X. H. Hu, Y. Tan, and J. L. Ping, *Eur. Phys. J. C* 81, 370 (2021).
- [33] X. H. Hu, and J. L. Ping, *Eur. Phys. J. C* 82, 118 (2022).
- [34] G. Yang, J. L. Ping, and J. Segovia, *Phys. Rev. D* 102, 054023 (2020).
- [35] Y. Tan, J. L. Ping, *Chin. Phys. C* 45, 093104 (2021).
- [36] J. Simons, *J. Chem. Phys.* 75, 2465 (1981).
- [37] E. Hiyama, A. Hosaka, M. Oka, J.M. Richard, *Phys. Rev. C* 98, 045208 (2018).
- [38] Q. Meng, E. Hiyama, K.U. Can, P. Gubler, M. Oka, A. Hosaka, H. Zong, *Phys. Lett. B* 798, 135028 (2019).
- [39] A. Valcarce, H. Garcilazo, F. Fernandez, and P. Gonzalez, *Rep. Prog. Phys.* 68, 965 (2005).
- [40] H. Garcilazo, T. Fernandez-Carame and A. Valcarce, *Phys. Rev. C* 75, 034002 (2007)